Colloid Polym Sci (2009) 287:481–485
DOI 10.1007/s00396-008-1992-x

SHORT COMMUNICATION

Hybrid ZnO/polymer thin films prepared by RF magnetron sputtering

Edit Pál · Torben Seemann · Volker Zöllmer · Matthias Busse · Imre Dékány

Received: 12 October 2008 / Revised: 17 December 2008 / Accepted: 18 December 2008 / Published online: 20 January 2009

Abstract Zinc oxide/poly(acrylic acid) (ZnO/PAA) multilayered hybrid films with different layer thicknesses were prepared by radio frequency magnetron sputtering. Zinc peroxide was used as precursor materials for the preparation of ZnO layers, since the zinc peroxide decomposes to ZnO during the film deposition. The films have a high transmittance in the visible region and exhibit visible photoluminescence emission. The band gap energy of the films—determined by the Tauc relationship—decreases with increasing layer thickness (3.40–3.36 eV) due to the increasing crystalline size of the ZnO particles. The morphological investigations showed that a real layered hybrid film structure formed.

Keywords ZnO · Polymer · Multilayer · Magnetron sputtering · Optical properties

E. Pál · I. Dékány
Department of Colloid Chemistry, University of Szeged,
Aradi vt. 1.,
Szeged 6720, Hungary

T. Seemann · V. Zöllmer · M. Busse
Fraunhofer Institute IFAM Manufacturing Advanced Materials,
Wiener Str. 12,
28359 Bremen, Germany

I. Dékány (✉)
Supramolecular and Nanostructured Materials Research Group
of the Hungarian Academy of Sciences, University of Szeged,
Aradi vt.1,
Szeged 6720, Hungary
e-mail: i.dekany@chem.u-szeged.hu

Introduction

Zinc oxide is a widely used n-type semiconductor oxide having a wide direct band gap (E_g=3.37 eV) and large excitation binding energy (60 meV) [1]. Many techniques are being used to prepare undoped and/or doped ZnO thin films such as layer-by-layer (LbL) self-assembly method [2], Langmuir–Blodgett technique [3, 4], spin coating [5], chemical vapour deposition [6], spray pyrolysis [7, 8] magnetron sputtering [9–15], etc. Owing to its favourable optical, electrical and catalytic properties, thin layers of ZnO are often utilised in solar cells [16–20] as gas sensors [21, 22], as photocatalyst [2] and as antireflective coating [23].

There are only few publications where other inorganic (silicate) [2] or organic (dyes) [24] material is applied in the thin films besides the ZnO to obtain 2D hybrid structures. ZnO/clay mineral and ZnO/polymer sandwich structures were prepared by Sebők et al. [25] using LbL method. The hybrid films were used as optical sensors to detect ethanol vapour.

Polymer layers such as polyimide [26], polytetrafluoroethylene [27], polyethylene and polypropylene [28] have also been successfully deposited by magnetron sputtering.

Since currently there is no available report on the deposition of ZnO/polymer hybrid structures by radio frequency (RF) magnetron sputtering, therefore we prepared ZnO/polymer structures applying the aforementioned technique. In the present work, the preparation of ZnO/poly(acrylic acid) hybrid structures by RF magnetron sputtering technique and the effect of the layer thickness and the ageing time on the optical (transmission, reflection and photoluminescence) and on the structural properties of films are described.

Experimental

Materials and sample preparation

Preparation of ZnO_2

Zinc oxide thin layer were prepared from ZnO_2, which decomposes to ZnO and O_2 due to heat (or plasma) treatment [29]. For the preparation of ZnO_2, 8.80 g zinc acetate dihydrate ($C_4H_6O_4Zn{\cdot}2H_2O$ Fluka, a.r.) was dissolved in the mixture of 52 ml demineralised water and 13.6 ml 30% hydrogen peroxide solution (H_2O_2, Reanal, a.r.) in a quartz beaker. The solution was placed into a water bath at 60 °C for 4 h and was irradiated with a xenon lamp (P=75 W) to obtain white ZnO_2 dispersion. At the half-time of the irradiation, 13.6 ml H_2O_2 was added to the mixture. The mean hydrodynamic particle diameter was 34 nm in the ZnO_2 suspension. The water was evaporated at 60 °C in air to obtain white ZnO_2 powder.

Preparation of the multilayered hybrid films

To deposit ZnO layers on glass substrates and silicon wafers, a quartz target covered with ZnO_2 was used. The ZnO_2 covered quartz target was prepared by spray coating technique using ZnO_2 suspension dispersed in ethanol (c= 1%, m/v). The thickness of the ZnO_2 layer on the quartz surface was ~7 μm. Power (100 W) and argon atmosphere at 1-Pa pressure were applied during the RF magnetron sputtering. The sputtering time was 30 min for one ZnO layer. The sputtering of a ZnO layer was followed by sputtering of a poly(acrylic acid) (PAA) layer. For the preparation of the PAA layers, quartz targets covered with PAA (M_W=100000, Sigma, a.r.) was used. The PAA covered target was prepared by spray coating using PAA dissolved in water (c=15%, m/v). The thickness of the PAA layer on the top of the quartz target was ~15 μm. The sputtering was done at 4-Pa pressure with 50-W power in argon atmosphere for 60 min to obtain one PAA layer. The substrates were rotated during the deposition to obtain uniform layers. One ZnO/PAA sandwich layers (bilayers) was built up from a ZnO and a PAA layer. During the preparation, the number of the ZnO/PAA bilayers (n) was varied (n=5, 10, 20).

Methods

The hydrodynamic diameter of the ZnO_2 particles was determined by dynamic light scattering using a Malvern Zetasizer Nano Series, Nano-ZS apparatus.

The optical (transmission and reflection) properties of the films were studied by a Micropack Nanocalc 2000 spectrophotometer. The reflection spectra of the films were measured in a special measuring cell equipped with a reflectance probe at the angle of detection of 0°. The photoluminescence emission spectra were recorded on a Horiba Jobin Yvon Fluoromax-4 type spectrofluorometer at 350-nm excitation wavelength.

X-ray diffraction (XRD) measurements were carried out on a Bruker D8 Advance diffractometer with Cu K_α radiation (40 kV, 30 mA). The Scherrer equation was used to determine the average particle diameter from the half-width of the corresponding diffraction peak:

$$d = \frac{k \times \lambda}{\beta \times \cos\Theta}, \tag{1}$$

where d is the average particle diameter, k is related to the crystallite shape, λ is the radiation wavelength, β is the line broadening ($\beta=\beta_s-\beta_o$, where β_s and β_o are the half-widths of the XRD peak of the sample and the silicon standard), and Θ is the Bragg angle.

The morphology of the films was examined by a Leo Gemini 1530 scanning electron microscope (SEM; InLens 3 kV 2 mm distance) and by a Digital Instruments Atomic Force Microscope Nanoscope III with a tapping type tip made of silicon (Veeco Nanoprobe Tips RTESP model, 125-μm length, 300 kHz).

Results and discussion

Optical properties

The optical UV–vis transmission property of films with different bilayer number prepared by RF magnetron sputtering was studied first. The films have high transmittance (T=75–95%) in the visible region (550–750 nm); furthermore, the transmission spectra show several minima due to the interference, as can be seen in Fig. 1a. The thickness of the films at different bilayer number can be calculated from the reflection spectra of the films using a computer simulation. This simulation calculates the intensities of the interference of the waves reflected from the surface of the film and from the substrate surface as the function of the wavelength using the method of complex amplitudes including the three-component Bruggeman formula [30]. Using this method, 423-, 622- and 1,426-nm thickness was obtained when n was 5, 10 and 20.

Slight red shift of the transmission spectra also can be observed, which indicates the decrease of band gap energy (E_g) of deposited semiconductor material. To verify our assumption, the E_g value of deposited films was calculated by the Tauc relationship:

$$a \times h \times \nu = A \times \left(h \times \nu - E_g\right)^n, \tag{2}$$

where α is the absorption coefficient, $h\nu$ is the photon energy, A is constant, E_g is the band gap energy and n=1/2

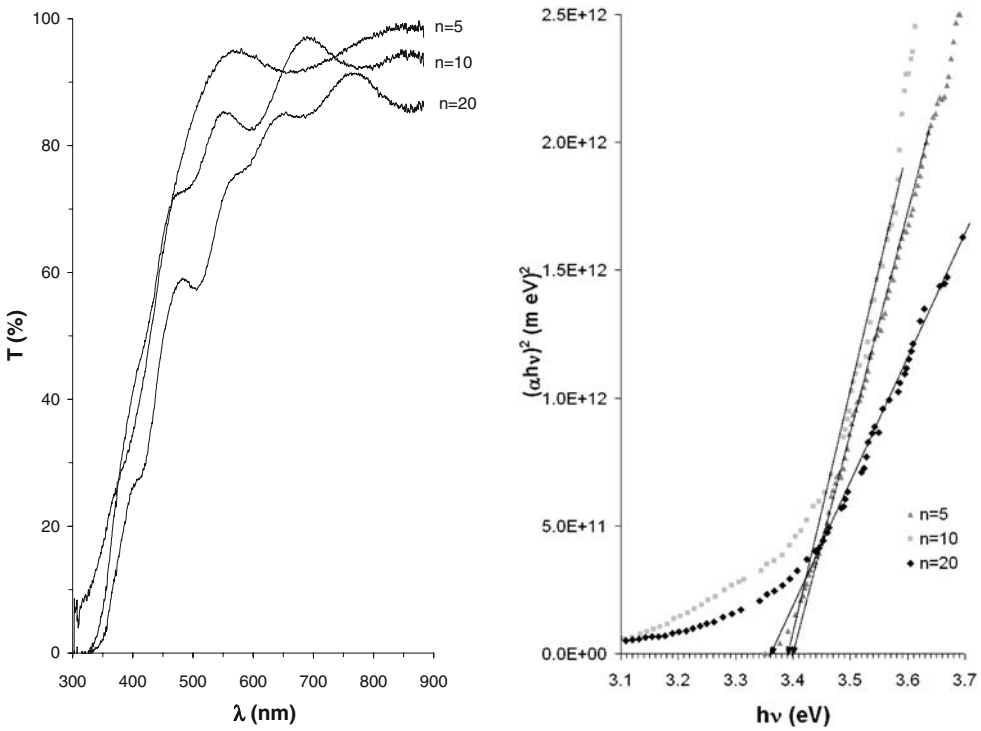

Fig. 1 **a** Transmission spectra of the ZnO/PAA hybrid films with different bilayer number. **b** Band gap energy determination of the films

[31]. The absorption coefficient, α, can be easily determined with the knowledge of the transmission and the reflection spectra of films from the following equation:

$$a = \frac{1}{d} \times \ln \frac{(1-R)}{T}, \tag{3}$$

where d is the layer thickness, R is the reflection of films and T is the transmittance of films [12].

The calculated E_g value of films with bilayer number of 5, 10 and 20 was $3.40\pm2\times10^{-3}$, $3.39\pm4\times10^{-3}$ and $3.36\pm3\times10^{-3}$ eV, respectively (Fig. 1b). The determined λ_g adsorption edge values of films at n=5, 10 and 20 are 364.7±0.2, 365.8±0.4 and 369.1±0.3 nm, respectively. The band gap energies of films at n=5 and 10 are similar; the difference between them is not significant. However, the slight decrease in the E_g can be determined at n=20. It can be explained by the increasing crystalline diameter, as it will be discussed later by results of XRD measurements.

The UV–vis transmission measurements were followed by photoluminescence studies of the films. The emission spectra of the films applying 350-nm excitation wavelength are presented in Fig. 2. Two emission peaks appear in every spectrum. One of them, located at 403 nm with high intensity, belongs to the glass support. In the case of the lowest bilayer number (n=5), a red emission peak appears at 669 nm. This visible emission peak shifts towards the higher energies with the increasing bilayer number and appears at 575 nm (green-yellow region) and 531 nm (green region) when n=10 and n=20, respectively. The visible emission peak in the red region related to the interstitial Zn (Zn_i) defects or Zn_i complexes, whilst the emission peak in the green and green-yellow regions could be assigned to the electron transition from the conduction band to the single electron oxygen vacancy (V_o^+) level [11].

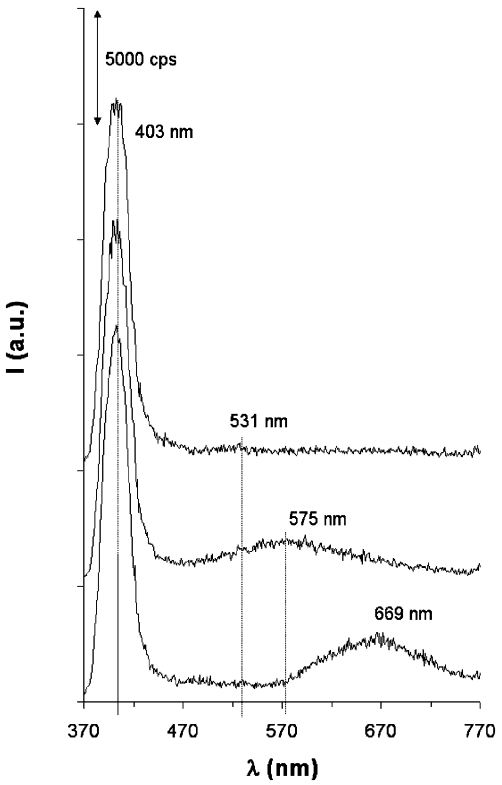

Fig. 2 Emission spectra of the ZnO/PAA films (λ_{ex}=350 nm)

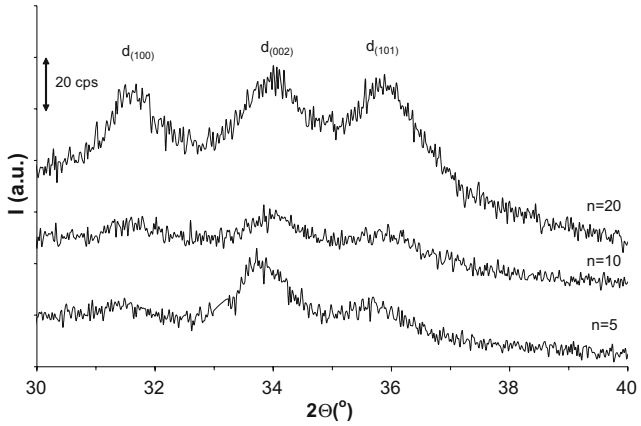

Fig. 3 XRD patterns of the films ZnO/PAA hybrid films

The shift of the visible emission can be explained by the ageing. The films spent different time in the sputtering chamber at ~120 °C during the deposition. Due to this heat treatment, the concentration of Zn defects decreases, whilst the concentration of O vacancies increases in the crystalline lattice of the ZnO [11].

Structural and morphological properties

The crystalline structures of the films were determined by XRD. Three diffraction peaks [$d_{(100)}$, $d_{(002)}$, $d_{(101)}$] of the ZnO appear on the XRD patterns of the films (Fig. 3). These peaks are characteristic of the hexagonal zincite crystalline structure (36-1451 JCPDS card). The XRD measurements confirmed that ZnO_2 decomposes due to the plasma treatment and ZnO layers are forming during the deposition. Using the Scherrer Eq. 1, the average diameter of the crystallites can be determined from the XRD patterns. The obtained diameter was 10.1, 13.3 and 17.2 nm when the bilayer number was 5, 10 and 20, respectively. Since the band gap energy is decreasing with the increasing particle size, it explains the red shift of the UV–vis transmission spectra and the decreasing band gap energies.

To examine the morphology of as-prepared films, SEM and atomic force microscopy (AFM) measurements were done. The cross-section SEM image of the film with bilayer number 5 is presented in Fig. 4a. The hybrid structure is well visualised by SEM, as the films build up from thicker ZnO layers (~60 nm) and thinner PAA layers (~30 nm). The thickness of the films can also be determined directly from the cross-section SEM images, which is 430, 640 and 1450 nm when the bilayer number is 5, 10 and 20, respectively. The thicknesses determined from the SEM images are in accordance with the thicknesses calculated from the transmittance spectra. The surface morphology of films was investigated by AFM. The AFM images are in

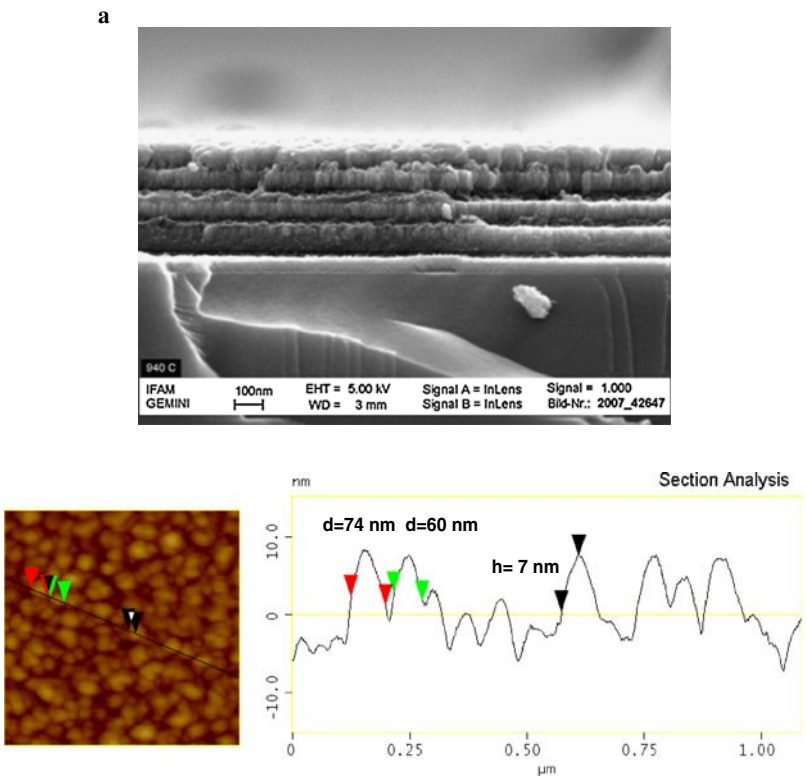

Fig. 4 **a** Cross-section SEM image of ZnO/PAA film **b** AFM image (1×1 µm) and cross-section AFM analysis of surface of ZnO/PAA film (n=5)

accordance with SEM images. A characteristic AFM image and cross-section analysis of the surface can be seen in Fig. 4b. The AFM image shows that the surface of the glass substrate is totally covered and the surface of the films is relatively flat. As it can be seen from the cross-section analysis, the average diameter of the aggregates is 65.4± 11.8 nm. The roughness also can be obtained from the AFM image, which is 24.15 nm for this sample.

Conclusion

ZnO/poly(acrylic acid) hybrid films with different bilayer number (n=5, 10, 20; different thickness) were prepared by RF magnetron sputtering. The films have high transmittance in the visible region. The band gap energy of hybrid films—determined by the Tauc relationship—decreases with increasing thickness (3.40–3.36 eV) because the mean diameter of the ZnO particles increases. The films show visible emission, and the emission peak shifts towards the higher energies with increasing bilayer number. This phenomenon could be explained by the deposition (ageing) time, whereas the concentration of the Zn and O defects in the crystalline lattice changes during the deposition. The XRD measurements confirmed that ZnO with zincite type crystalline structure forms from the ZnO_2 precursor during the deposition. SEM investigations represent that a real layered hybrid structures developed on the surface of the substrates.

Acknowledgement The authors are very thankful for the financial support of the National Scientific Fund (OTKA) no. K73307.

References

1. Ma X, Liu A, Xu H, Li G (2007) Colloid Polym Sci 285:1631
2. Szabó T, Németh J, Dékány I (2004) Coll Surf A: Physicochem Eng Aspects 230:23
3. Singh S, Srinivasa RS, Talwar SS, Major SS (2007) Thin Solid Films 515:8714
4. Naszályi L, Deák A, Hild E, Ayral A, Kovács AL, Hórvölgyi Z (2006) Thin Solid Films 515:2587
5. Zhang LZ, Tang GQ (2004) Opt Mater 27:217
6. Gulino A, Fragala I (2002) Chem Mater 14:116
7. Yoshida MM, Delgado FP, López WE, Andrade E (2000) Thin Solid Films 376:99
8. Lucio-López MA, Luna-Arias MA, Maldonado A, Olvera ML, Acosta DR (2006) Sol Energy Mater Sol Cells 90:733
9. Huang B, Li J, Wu Y, Guo D, Wu S (2008) Mater Lett 62:1316
10. Dang WL, Fu YQ, Luo JK, Flewitt AJ, Milne WI (2007) Superlattices Microstruct 42:89
11. Xing GZ, Yao B, Cong CX, Yang T, Xie YP, Li BH, Shen DZ (2008) J Alloys Compd, 457:36
12. Lan W, Liu Y, Zhang M, Wang B, Yan H, Wang Y (2007) Mater Lett 61:2262
13. Hsieh PT, Chen YC, Kao KS, Wang CM (2007) Physica B 392:332
14. Li LJ, Deng H, Dai LP, Chen JJ, Yuan QL, Li Y (2008) Mater Res Bull 43:1456
15. Mandal S, Singha RK, Dhar A, Ray SK (2008) Mater Res Bull 43:244
16. Lee JC, Kang KH, Kim SK, Yoon KH, Park IJ, Song J (2000) Sol Energy Mater Sol Cells 64:185
17. Gao Y, Nagai M (2006) Langmuir 22:3936
18. Ravirajan P, Peiró AM, Nazeeruddin MK, Graetzel M, Bradley DDC, Durrant JR, Nelson J (2006) J Phys Chem B 110:7635
19. Rusu M, Eisele W, Würz R, Ennaoui A, Lux-Steiner MCh, Niesen TP, Karg F (2003) J Phys Chem Solids 64:2037
20. Olson DC, Piris J, Collins RT, Shaheen SE, Ginley DS (2006) Thin Solid Films 496:26
21. Németh Á, Horváth E, Lábadi Z, Fedák L, Bársony I (2007) Sens Actuators B 127:157
22. Sonawane YS, Kanade KG, Kale BB, Aiyer RC (2008) Mater Res Bull 43:2719
23. Lee YJ, Ruby DS, Peters DW, Mckenzie BB, Hsu JWP (2008) Nano lett 8:1501
24. Oekermann T, Yoshida T, Tada H, Minoura H (2006) Thin Solid Films 511–512:354
25. Sebők D, Szendrei K, Szabó T, Dékány I (2008) Thin Solid Films 516:3009
26. Choukourov A, Hanus J, Kousal J, Grinevich A, Pihosh Y, Slavínská D, Biederman H (2006) Vacuum 81:517
27. Biedermann H (2000) Vacuum 59:594
28. Pihosh Y, Biedermann H, Slavinska D, Kousal J, Choukourov A, Trchova M, Mackova A, Boldyreva A (2006) Vacuum 81:32
29. Sun M, Hao W, Wang C, Wang T (2007) Chem Phys Lett 443:342
30. Theiß W (2007) Surface Sci Rep 29:91
31. Tauc J (1974) Amorphous and liquid semiconductor. Plenum, New York